Molecular target and projectile angular scattering effects in stopping power and charge exchange at low-to-intermediate projectile energies

R. Cabrera-Trujillo, Y. Öhrn, John R. Sabin, and E. Deumens
Quantum Theory Project, Departments of Physics and Chemistry, University of Florida, Gainesville, Florida 32611-8435
(Received 1 June 2001; published 3 January 2002)

We analyze the implications of the molecular structure of a target and the angular scattering effects on projectile-target collisions within the Electron-Nuclear Dynamics (END) approach. We show the suitability of the END method for the analysis of molecular scattering processes such as differential cross sections, charge exchange, and energy loss as required for the study of the stopping cross section. As a consequence of these effects, we show that the rovibronic energy loss becomes of greatest importance at low projectile energies. Furthermore, we find that the Bragg additivity rule and the linear-velocity dependence of the stopping cross section are not fulfilled at low projectile energies. Finally, we analyze the differences in the scattering processes for molecular and atomic targets, and show that in a transmission experiment with small exit window, the acceptance angle corresponds to different impact parameter selection for molecular targets than for atomic ones. Thus, the measured stopping cross section becomes a function of the acceptance angle of the experimental setup. We present results for hydrogen beams on H_2 and N_2 gas targets.

DOI: 10.1103/PhysRevA.65.024901 PACS number(s): 34.50.Bw, 34.70.+e

It has been known since the beginning of the last century that the interposition of an absorbing medium in a beam of charged particles introduces processes such as energy loss and angular scattering of the projectiles. However, given the many-body character of the interactions, it has been difficult to obtain from first principles, quantitative or qualitative accounts of the energy loss, charge exchange, and differential cross section at low-projectile velocities. For molecular targets, there is the additional problem of deviation from the additivity of the atomic contributions to the stopping cross section (Bragg's rule) [1,2]. This deviation, due to chemical bonding, becomes more pronounced in the low projectile energy region where collision times are longer and the projectile-target system tends to form a quasimolecule. Although there exist a few theoretical studies that attempt to account for the effect of different bond types on the stopping by hydrocarbons using simple models [3–7], little is known about the energy deposition in collisions involving molecules. Furthermore, rotational and vibrational contributions of the molecule are neglected by Bragg's rule at low collision energies, where these effects are important. Both experimental and theoretical studies of these effects are scarce, and few reviews of the subject exist [2,7–9].

The definition of the stopping cross section is

$$S(E_p) = \int \Delta E \frac{d\sigma}{d\Omega} d\Omega \tag{1}$$

with $d\Omega = \sin(\theta) d\theta d\varphi$ being the differential solid angle for the scattered particle, ΔE the energy loss of a projectile with initial energy E_p, and $d\sigma/d\Omega$ the direct differential cross section. In Eq. (1), one should include integration over all the scattering angles, including backward scattering. In a transmission experiment, however, the detected particles are limited to those that are deflected with such an angle that they reach the exit window of the experimental setup in a forward direction, thus defining an acceptance angle θ_a. This problem has been discussed recently by Semrad *et al.* [10] within an electron-gas model. However, the stopping cross section, for the same acceptance angle θ_a, can be shown to be different for a molecular or atomic target. These problems become of fundamental importance and require an *ab initio* treatment to fully understand the dynamics of the collision.

Our approach is based on the time-dependent variational principle [11], which requires that the quantum action be stationary under variations of the wave function over a subspace. This approach is called electron-nuclear dynamics (END). Details of END have been reported elsewhere [11] and it is implemented in the ENDyne program package [12].

The END approach requires specification of the initial conditions of the system in a Cartesian laboratory frame. For the case of atomic projectiles, we need to consider only the initial orientations of the molecular target. The molecular target is placed arbitrarily with its center of mass at the origin of a Cartesian coordinate system. The projectile beam is aligned parallel to the z axis at a distance b (impact parameter) from it. As an experiment using a gaseous target will sample all target orientations, we orientationally average our results by integrating over Euler angles. For homonuclear diatomic molecules, we consider three orientations of the target along the Cartesian axis. These orientations yield a coarse set of grid points that we use for rotational averaging. Initially the projectile is placed at a distance of 30 a.u. from the x-y plane, with a kinetic energy ranging from 10 eV/amu to 25 keV/amu. The target is chosen to be in its electronic ground state and equilibrium geometry as determined in the computational basis set at the self-consistent-field level. The electronic basis set used, consists of $5s$ and $2p$ uncontracted Gaussian basis for each hydrogen atom [13] with the addition of a diffuse s and p orbital. The impact parameter b takes values from 0.0 to 15.0 a.u. For each trajectory, the dynamics was studied until the projectile reached a distance of 30 a.u. past the x-y plane. At the completion of each END trajectory, we obtain the final nuclear positions, velocities, the atomic electron populations, and the wave functions. Further details

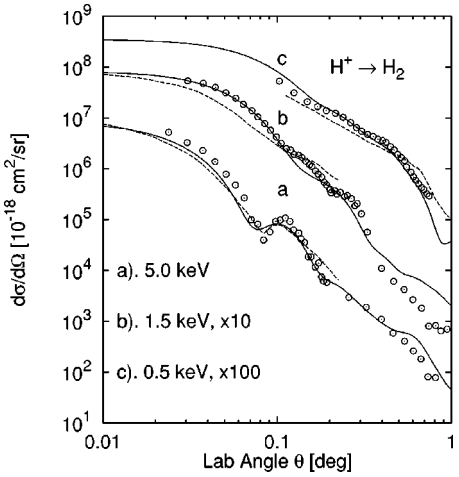

FIG. 1. Orientationally averaged direct differential cross section for H^+ colliding with H_2 as a function of the laboratory scattering angle for projectiles energies of 0.5, 1.5, and 5.0 keV/amu. The experimental points (○) are from Gao *et al.* [18]. The theoretical results (dashed line), as obtained by the diatoms-in-molecule method (close coupling) reported in Ref. [18], are shown for comparison.

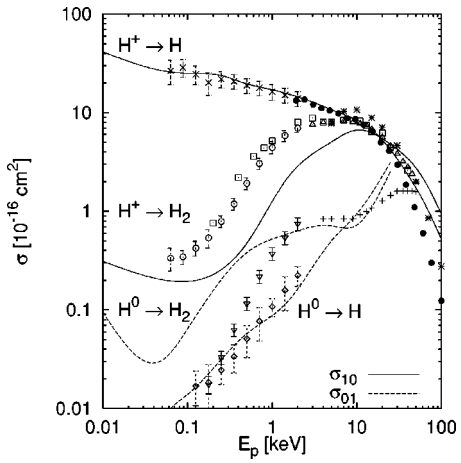

FIG. 2. Electron capture σ_{10} and electron loss σ_{01} cross sections for H colliding with H_2. For comparison we show the results for σ_{10}, obtained for the atomic case [25]. The experiment data are from Ref. [19] (×), Ref. [20] (●) for $H^+ \rightarrow H$; Ref. [19] (◇) for $H^0 \rightarrow H$; Ref. [19] (○), Ref. [21] (□), Ref. [22] (△), Ref. [23] (*) for $H^+ \rightarrow H_2$; Ref. [24] (+), Ref. [19] (▽) for $H^0 \rightarrow H_2$.

of the procedure for obtaining energy losses and stopping cross sections within the END approach can be found in Refs. [15,16].

From Eq. (1), the stopping cross section requires calculations of the direct differential cross section and energy loss. Since we are describing the dynamics of the nuclei as classical particles by invoking the narrow width limit for the nuclear wave packets, semiclassical corrections are needed to describe nuclei quantum interference. To this end, we have implemented [14,15] the Schiff approximation [16] for small scattering angles, thus taking into account quantum effects. The Schiff approximation includes all terms in the Born series, and treats the rainbow and glory angles in a single approach.

As examples, we consider hydrogen beams impinging on gaseous H_2 and N_2 targets. In Fig. 1, we show the orientationally averaged direct differential cross section for proton projectiles colliding with molecular hydrogen for 0.5, 1.5, and 5.0 keV energies as a function of the laboratory angle. In the same figure, we compare with the theoretical results of Kimura obtained with the close-coupling method [17] (dashed line), and with the experimental data of Gao *et al.* [18]. The agreement between the theory and experiment is reasonably good, considering the complexity of the collision system. In particular, note that the forward scattering is described correctly as a result of the correct dynamics. For larger scattering angles, the lack of averaging over more target orientations and the high probability for ionization makes our results in only fair agreement with experiment.

In Fig. 2, we show the results for the total orientationally averaged electron capture σ_{10} and electron loss σ_{01}, and cross sections for a hydrogen beam colliding with H_2 at energies ranging from 10 eV/amu to 25 keV/amu and we compare with representative experimental data [19–24]. In order to illustrate the differences due to chemical bonding (Bragg's rule [1]), we also present the results for atomic hydrogen targets [25]. Note that our results are proportionally lower for $H^+ \rightarrow H_2$ than those reported in Refs. [19,21] that were normalized to 6.95×10^{-16} cm^2 at $E_p = 2$ keV. Normalizing in the same manner, our results agree well with the experiment.

The energy loss, as needed in Eq. (1) is calculated as a function of the scattering angle, from the final kinetic energy of the projectile.

The components necessary to carry out the integral in Eq. (1) are now in place. To calculate the stopping cross section, the integral is carried out for $0 \leqslant \Omega \leqslant 4\pi$, that is, over all solid angles. However, as Semrad [10] has pointed out, an experiment is confined by the acceptance angle of its detector, and so, to compare to a measured stopping cross section, we should integrate Eq. (1) only over the range corresponding to the acceptance angle used in experiments. To investigate the effects of the acceptance angle (θ_a) on a measured stopping cross section $S_M(E_p)$, we calculate the acceptance angle dependent, orientationally averaged stopping cross section $S_M(E_p, \theta_a)$, which is smaller than $S(E_p)$, by carrying out the integral in Eq. (1) up to a scattering angle θ_a, corresponding to the acceptance angle in an experiment. In Fig. 3, we present $S_M(E_p, \theta_a)$ calculated for various projectile energies as a function of the acceptance angle $0 \leqslant \theta_a \leqslant 100°$ for atomic hydrogen colliding with H and H_2. In the same figure, we show the electronic energy loss, which we obtain by subtracting the nuclear and rovibrational energy loss from the total energy loss. Thus, for large angles and low projectile energies, we note that the increase in the contribution is due to rovibrational energy loss and nuclear energy loss, which corresponds to close collisions with the target. These contributions of the electronic and rovibrational excitations become more important in a collision with large complex systems [26].

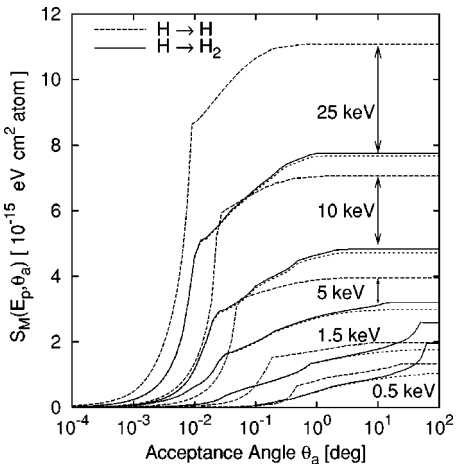

FIG. 3. Stopping cross section per atom as a function of the acceptance angle θ_a for atomic hydrogen colliding with atomic and molecular hydrogen for projectile energies of 0.5, 1.5, 5.0, 10.0, and 25.0 keV in ascending order. The solid line represents the total stopping cross section for the molecular target and the short-dashed line is the electronic stopping cross section (see text). The long-dashed line is the total stopping cross section for the atomic target for the same projectile energies.

From Fig. 3, we note that the higher the projectile energy, the steeper the curve, since for high projectile energies, the projectile moves in a nearly rectilinear trajectory. However, this is not the case at low energies, where large angular scattering processes have a higher probability. We note that for the atomic target, a higher total stopping cross section is obtained for the same scattering angle when compared to the molecular case. Thus, care must be taken when comparing with experiment for low projectile energy.

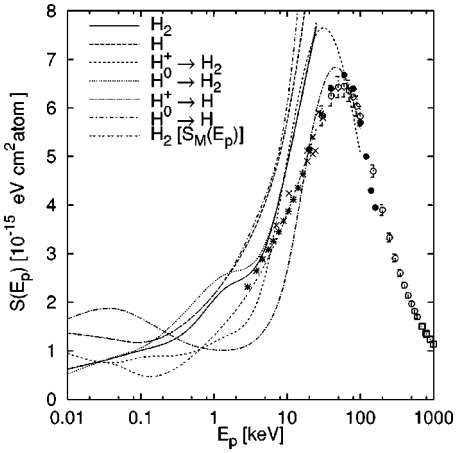

FIG. 4. Total stopping cross section for H and H_2 targets for hydrogen beams. Solid line (hydrogen beam on H_2), long-dashed line (hydrogen beam on H), short-dashed line ($H^+ \rightarrow H_2$), dotted line ($H \rightarrow H_2$), dot–long-dash line ($H^+ \rightarrow H$), dot–short-dash line ($H \rightarrow H$), and double short-dash line is the acceptance angle result $S_M(E_p)$ (see text). Note the difference between the atomic and molecular case, particularly for proton projectiles. The experiments are taken from Ref. [27] (∗), Ref. [28] (○), Ref. [29] (●), Ref. [30] (□), and Ref. [31] (×).

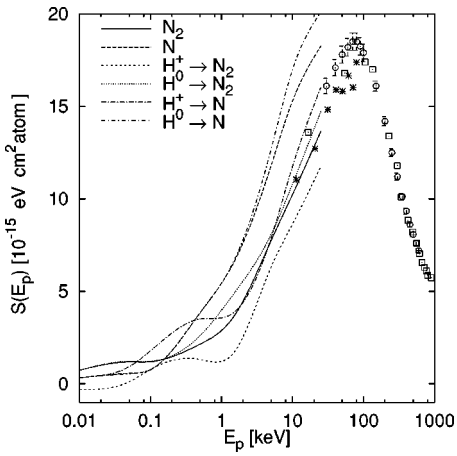

FIG. 5. Total stopping cross section for N and N_2 targets for a hydrogen beam. Labels are the same as in Fig. 4.

In Figs. 4 and 5, we show the total stopping cross section for molecular hydrogen and nitrogen targets, respectively, as a function of the projectile energy and compare with the experimental data available [27–31] when we include all the scattering angles according to Eq. (1). The results were obtained by averaging the contributions of proton projectiles and neutral-hydrogen projectiles on H_2 and N_2 by following the charge state average approach as devised by Dalgarno and Griffing [32]. The method consists of calculating the charge state fraction of protons F^+ and hydrogen atoms F^0 in the beam by means of the electron-capture cross section σ_{10} and the electron-loss cross section σ_{01}, and, thus $S(E_p)=F^+S^+ + F^0S^0$. Here, we assume that the probability of forming H^- is negligible. In the same figures, we show the orientationally averaged contributions to $S(E_p)$ for H^+ and H^0 projectiles on the molecular targets as well as the equivalent results for the atomic case [25]. We note that the results for the molecular target are lower than those predicted by Bragg's rule. For the case of molecular nitrogen, the results are inverted at energies lower than 100 eV/amu due to the contributions of the rovibrational channel, while for the molecular hydrogen case, the stopping cross section is lower than the atomic, since the nuclear energy loss is larger for the atomic case due to the similar masses of the projectile and target. For both H_2 and N_2 targets the deviation from Bragg's rule is more pronounced at low energies with H^+ projectiles. From these results, we note that the velocity dependence of the stopping cross section at low projectile energy is not linear, a result previously reported [25].

Following the impact parameter selection scheme of Semrad *et al.* [10] in Eq. (1), we obtain the molecular stopping cross section $S_M(E_p)$ as a function of projectile energy that is in good agreement with the experimental data available, as shown in Fig. 4 for the case of a hydrogen beam colliding with molecular hydrogen, confirming the acceptance angle selectivity of the experimental device.

In summary, from the present calculations it is apparent that (i) the molecular bond plays an important role in energy loss processes and (ii) electronic and rovibrational excita-

tions as well as acceptance angle conditions become important for large scattering angles.

This work was supported in part by CONACyT-Mexico (R.C.T.), by the NSF (Grant No. CHE-9732902 to N.Y.O. and CHE-9974385 to J.R.S.), by the ONR (Grant No. N0014-97-1-0261 to N.Y.O. and N000149610707 to J.R.S.), by the IBM SUR program for 1999, and by a grant of a 134-node SP from MHPCC.

[1] W.H. Bragg and R. Kleeman, Philos. Mag. **10**, 305 (1918).
[2] D.I. Thwaites, Radiat. Res. **95**, 495 (1983).
[3] J.R. Sabin and J. Oddershede, Nucl. Instrum. Methods Phys. Res. B **27**, 280 (1987).
[4] J. Oddershede and J.R. Sabin, Nucl. Instrum. Methods Phys. Res. B **42**, 7 (1989).
[5] S.A. Cruz, J. Soullard, and R. Cabrera-Trujillo, Nucl. Instrum. Methods Phys. Res. B **83**, 5 (1993).
[6] R. Cabrera-Trujillo, S. Cruz, and J. Soullard, Nucl. Instrum. Methods Phys. Res. B **93**, 166 (1994).
[7] D. Powers, Acc. Chem. Res. **13**, 433 (1980).
[8] D.I. Thwaites, Nucl. Instrum. Methods Phys. Res. B **23**, 293 (1987).
[9] A.V. Phelps, J. Phys. Chem. Ref. Data **19**, 653 (1990).
[10] D. Semrad *et al.*, Nucl. Instrum. Methods Phys. Res. B **164-165**, 284 (2000).
[11] E. Deumens, A. Diz, R. Longo, and Y. Öhrn, Rev. Mod. Phys. **66**, 917 (1994).
[12] E. Deumens *et al.*, ENDyne version 2.7 Software for Electron Nuclear Dynamics, Quantum Theory Project, (University of Florida, 1998).
[13] T.H. Dunning, J. Chem. Phys. **90**, 1007 (1989).
[14] R. Cabrera-Trujillo, J.R. Sabin, Y. Öhrn, and E. Deumens, Phys. Rev. A **61**, 032719 (2000).
[15] R. Cabrera-Trujillo, Y. Öhrn, E. Deumens, and J.R. Sabin, Phys. Rev. A **62**, 052714 (2000).
[16] L.I. Schiff, Phys. Rev. **103**, 443 (1956).
[17] M. Kimura, J. Chapman, and N.F. Lane, Phys. Rev. A **33**, 1619 (1986).
[18] R.S. Gao *et al.*, Phys. Rev. A **44**, 5599 (1991).
[19] M.W. Gealy and B. Van-Zyl, Phys. Rev. A **36**, 3091 (1987).
[20] G.W. McClure, Phys. Rev. **148**, 47 (1966).
[21] J.B. Hasted, Proc. R. Soc. London, Ser. A **227**, 466 (1955).
[22] R. K. Curran and T. M. Donahue, Tech. Report ONR-8, Office of Naval Research (unpublished).
[23] M.E. Rudd *et al.*, Phys. Rev. A **28**, 3244 (1983).
[24] P.M. Stier and C.F. Barnett, Phys. Rev. **103**, 896 (1956).
[25] R. Cabrera-Trujillo, J.R. Sabin, Y. Öhrn, and E. Deumens, Phys. Rev. Lett. **84**, 5300 (2000).
[26] T. Kunert and R. Schmidt, Phys. Rev. Lett. **86**, 5258 (2001).
[27] R. Golser and D. Semrad, Nucl. Instrum. Methods Phys. Res. B **69**, 18 (1992).
[28] H.K. Reynolds, D.N. Dunbar, W.A. Wenzel, and W. Whaling, Phys. Rev. **92**, 742 (1953).
[29] S.K. Allison, J. Cuevas, and M. Garcia-Munoz, Phys. Rev. **127**, 792 (1962).
[30] G. Reiter, N. Kniest, E. Pfaff, and G. Clausnitzer, Nucl. Instrum. Methods Phys. Res. B **44**, 399 (1990).
[31] J.A. Phillips, Phys. Rev. **90**, 532 (1953).
[32] A. Dalgarno and G.W. Griffing, Proc. R. Soc. London, Ser. A **232**, 423 (1955).